Polarization rotator using a hybrid aligned nematic liquid crystal cell

Fuzi Yang

Chemistry Department, Tsinghua University, Beijing 100084, China

Lizhen Ruan, S. A. Jewell and J. R. Sambles

Thin Film Photonics, School of Physics, University of Exeter, Stocker Road, Exeter EX4 4QL, United Kingdom

Abstract: Using both direct mathematical analysis and numerical modeling based on the predictions by Jones [1] it is shown that if the director in a liquid crystal cell is in a plane which lies at 45° to the incident polarization, then, for normally incident light, the transmission signal which conserves polarization will always have a phase difference of π/2 from the transmission signal of the orthogonal polarization. This is independent of the director profile in the plane, the cell thickness, the anisotropy of the liquid crystal refractive index and the optical parameters of other isotropic layers in the cell. Based on this realization a hybrid aligned nematic liquid crystal cell has been tested as a thresholdless voltage-controlled polarization rotator. By using a quarter-wave plate to compensate for the phase difference between the two orthogonal output polarizations a simple liquid crystal spatial light modulator has been realized.

OCIS codes: (230.6120) Spatial light modulators; .(260.5430) Polarization; (230.3720) Liquid-crystal devices

---

References and links

1. R. C. Jones, "A new calculation for the treatment of optical systems, III. The Sohncke theory of optical activity," J. Opt. Soc. Am. **31,** 500-503 (1941).
2. J. L. Horner and P. D. Gianino, "Phase-only matched filtering," Appl. Opt. **23** 812-816 (1984).
3. J. A. Davis, D. E. McNamara and D. M. Cottrell, "Encoding complex diffractive optical elements onto a phase-only liquid-crystal spatial light modulator," Opt. Eng. **40,** 327-329 (2001).
4. L. Hu, L. Xuan, Y. Liu, Z. Cao, D. Li, and Q. Mu, "Phase-only liquid crystal spatial light modulator for wavefront correction with high precision," Opt. Express **12,** 6403-6409 (2004).
5. V. Arrizon, G. Mendez and D. Sanchez-de-La-Llave, "Accurate encoding of arbitrary complex fields with amplitude-only liquid crystal spatial light modulator," Opt. Express **13,** 7913-7927 (2005).
6. M. Stalder and M. Schadt, "Linearly polarized light with axial symmetry generated by liquid-crystal polarization converters," Opt. Lett. **21,** 1948-1950 (1996).
7. Z. Zhuang, S.-W. Suh and J. S. Patel, "Polarization controller using nematic liquid crystals," Opt. Lett. **24,** 694-696 (1999).
8. Yu T-C and Lo Y-L, "Using a new liquid-crystal polarization modulator for a polarimetric glucose sensor," SPIE Proc. **5852**, 21-27 (2005).
9. J. Remenyi, P. Varhegyi, L. Domjan, P. Koppa and E. Lorincz, "Amplitude, phase, and hybrid ternary modulation modes of a twisted-nematic liquid-crystal display at ~400 nm," Appl. Opt. **42**, 3428-3434 (2003).
10. J. S. Jang and D. H. Shin, "Optical representation of binary data based on both intensity and phase modulation with a twisted-nematic liquid-crystal display for holographic digital data storage," Opt. Lett. **26,** 1797-1799 (2001).
11. J. A. Davis, D. E. McNamara, D. M. Cottrell and T. Sonehara, "Two-dimentional Polarization Encoding with a Phase-only Liquid Crystal Light Modulator," Appl. Opt, **39**, 1549-1554 (2000).
12. J. Nicolas, J. Campos and M. J. Yzuel, "Phase and amplitude modulation of elliptic polarization states by nonabsorbing anisotropic elements: application to liquid-crystal devices," J. Opt. Soc. Am. A **19,** 1013-1020 (2002).

---

1. Introduction

Spatial light modulators (SLM) are very important optical devices finding use in areas such as optical image processing, adaptive optics and optical communication etc. Often a core component in a SLM is a liquid crystal cell. This is because liquid crystals have high optical anisotropy and are easily controlled with low-voltages. Not surprisingly then the liquid crystal spatial light modulator (LC-SLM) has been an active area of study for some time [2-12].

Due to the character of optical radiation there may be three kinds of spatial light modulation: phase, amplitude and polarization. Ideally phase SLMs change only the spatial distribution of the phase of the radiation [2-4], amplitude SLMs ideally give only amplitude changes of the beam [5] and polarization SLMs modulate just the polarization distribution [6,7]. Combination modulators may also be found [8-10,12]. By comparison with phase and amplitude LC-SLMs rather little work has been presented on polarization LC-SLMs, although commercial liquid crystal polarization rotators have been realized. For the polarization-only modulator a polarization rotator is the essential requirement with generally linearly polarized output and well defined polarization angle controlled by low voltage. In addition it is important that the intensity of the output is not modulated with the polarization. The essentials of such a device have previously been reported through the use of a parallel aligned liquid crystal cell sandwiched between two quarter-wave plates [11]. In such an arrangement, the fast axes of the two quarter-wave plates are crossed and the extra-ordinary axis of the liquid crystal cell is set at 45° between the two and the angle of rotation of the polarized light is controlled through the application of a voltage across the cell. However, the theoretical analysis in [11], using a Jones matrix, treats the liquid crystal cell as a uniform block with the same director tilt angle and fixed twist angle (45°) through the whole cell. In actual fact, even for a parallel aligned liquid crystal cell, which is studied in [11], this situation is only true for no applied field. When an electrical field is applied the director tilt angle will vary through the whole cell in a plane at a fixed twist angle of 45°.

The polarization rotator study presented here differs from the previous case in several ways. Firstly, the need for the incident quarter-wave plate to convert the linearly-polarised light into circularly-polarised light is removed for the following reason. Consider a liquid crystal cell in which the director (i.e. the average molecular direction) always lies in a plane at 45° to the plane of polarization of the incident light. Because of the uniaxial character of the liquid crystal this will introduce polarization conversion and the transmitted wave will contain, in general, both the input polarization and a component at right-angles to it. What is here appreciated, and crucial to all that follows, is that these two output components will **always** have a phase difference of $\pi/2$, as was predicted by Jones [1] in the case of a single uniform block. This phase difference is totally independent of the director profile in the plane, the cell thickness, the anisotropy of the liquid crystal index or the optical parameters of other isotropic layers in the cell. If this phase difference, $\pi/2$, is compensated by a suitable optical element, for example a quarter-wave plate, this results in the final output wave having in-phase orthogonal polarization components. Now as a voltage is applied the director reorients and the amount of polarization conversion changes with voltage, leading to different amplitudes in the orthogonal polarizations. Thus, the final output after the quarter-wave plate will be linearly polarized and of constant intensity with its polarization direction rotating in space as the voltage is varied: an ideal polarization rotator.

Based on the analyses mentioned above a further difference arises from the choice of liquid crystal geometry. This study uses a hybrid aligned nematic (HAN) cell, which always has a varying director tilt angle through the cell. Such an alignment allows the director to lie in a plane at 45° to the input polarization but, crucially, it has a thresholdless response to an applied field which allows a greater control over the polarization rotation angle. For comparison, we also present results for a single quarter-wave plate rotator with a parallel-aligned liquid crystal cell as the active electro-optical component. In this case the director tilt angle only varies through the cell when an external electric field applied. Finally, we model the optical response of the system using a computational model based on a 4×4 Berreman

matter which allows a more thorough treatment of the optical properties of the system than is achievable through the use of the Jones matrix method used previously.

2. Analysis

Figure 1 shows a director of the nematic liquid crystal in the lab-system, O-XYZ. ZOX is the incident plane. The plane ZOA contains the director **n** which has tilt angle θ and twist angle ϕ (= 45°). The uniaxial character of the liquid crystal is specified by the two indices n_o and n_e, the ordinary (perpendicular) and extraordinary (parallel) indices respectively. The effective extraordinary index n_e' relative to the incident polarization is then given by

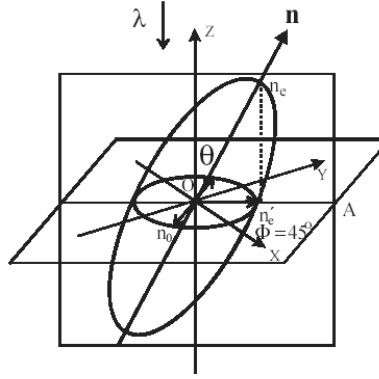$$n_e' = \frac{n_e n_o}{\sqrt{n_e^2 \cos^2\theta + n_o^2 \sin^2\theta}} \tag{1}$$

Fig. 1. The director in the lab-system, O-XYZ.

Consider dividing the liquid crystal, of thickness d, into N slices of thicknesses d_1, d_2, .., d_N, tilt angles θ_1, θ_2, .., θ_N, and effective extraordinary indices $n_e'^{(1)}$, $n_e'^{(2)}$, .., $n_e'^{(N)}$, respectively. For an x-polarized incident beam, defined as $x_0 = 1$ and $y_0 = 0$, after passing through the first thin slab of liquid crystal, ignoring the very weak reflection, the new electric field vector becomes

$$x_1 = \frac{1}{2}[e^{i\frac{2\pi}{\lambda}n_e'^{(1)}d_1} + e^{i\frac{2\pi}{\lambda}n_o d_1}] = \cos[\frac{\pi}{\lambda}(n_e'^{(1)} - n_o)d_1] \cdot e^{i[\frac{\pi}{\lambda}(n_e'^{(1)}+n_o)d_1]} = A_{x_1} e^{i\Phi_{x_1}},$$

$$y_1 = \frac{1}{2}[e^{i\frac{2\pi}{\lambda}n_e'^{(1)}d_1} - e^{i\frac{2\pi}{\lambda}n_o d_1}] = \sin[\frac{\pi}{\lambda}(n_e'^{(1)} - n_o)d_1] \cdot e^{i[\frac{\pi}{\lambda}(n_e'^{(1)}+n_o)d_1+\frac{\pi}{2}]} = A_{y_1} e^{i\Phi_{y_1}},$$

where the phase difference between the output y and x polarizations is clearly $\Phi_{y_1} - \Phi_{x_1} = \frac{\pi}{2}$.

To consider the propagation through the second thin slice redefine the phase angle so that

$x_1 = A_{x_1}$, $y_1 = A_{y_1}e^{i\frac{\pi}{2}}$ and $A_{y_1} = \sqrt{1 - A_{x_1}^2}$. It follows that

$$x_2 = \frac{1}{2}[(x_1 + y_1)e^{i\frac{2\pi}{\lambda}n_e'^{(2)}d_2} + (x_1 - y_1)e^{i\frac{2\pi}{\lambda}n_o d_2}] = A_{x_2} e^{i\Phi_{x_2}},$$

$$y_2 = \frac{1}{2}[(x_1 + y_1)e^{i\frac{2\pi}{\lambda}n_e'^{(2)}d_2} - (x_1 - y_1)e^{i\frac{2\pi}{\lambda}n_o d_2} = A_{y_2} e^{i\Phi_{y_2}}] \text{ with } A_{y_2} = \sqrt{1 - A_{x_2}^2} \text{ and}$$

$$\Phi_{x_2} = \frac{\pi}{\lambda}[n_e'^{(2)} + n_o]d_2, \Phi_{y_2} = \frac{\pi}{\lambda}[n_e'^{(2)} + n_o]d_2 + \frac{\pi}{2}.$$

Once again the phase difference between the output *y*- and *x* polarizations is $\pi/2$. This procedure can be continued through all N slices so that the final transmitted wave will have

$$\Phi_x = \Phi \text{ and } \Phi_y = \Phi + \pi/2, \text{ where } \Phi = \frac{\pi}{\lambda} \sum_{n=1}^{N} (n_e^{\prime(n)} + n_o) d_n \text{ , giving}$$

$$\Phi = \frac{\pi}{\lambda} n_o [d + n_e \int_o^d \frac{dz}{\sqrt{n_e^2 \cos^2 \theta(z) + n_o^2 \sin^2 \theta(z)}}] \tag{2}$$

If the incoming radiation is purely *y*-polarized then the phase difference between the *y* and *x* polarized output beams is now -$\pi/2$. It is very clear that this $\pi/2$ phase difference is independent of the varying director tilt angle, the cell thickness, the anisotropy of the liquid crystal and the isotropic layers. The analysis used above is based on the same principle as the Jones matrix to demonstrate the effect from a series of small slabs. It should be noted that reflections at the liquid crystal- isotropic layer interface, which is ignored in this Jones matrix treatment, may have an effect but, as is shown experimentally, this is rather small.

3. Modeling

Several numerical models have been evaluated to confirm the expected $\pi/2$ phase difference. The general sample configuration for modeling is a HAN geometry of liquid crystal material sandwiched between two glass plates. At a radiation wavelength of $\lambda = 632.8$ nm (He-Ne laser) the refractive index for glass is set at $n_g = 1.5170$. To compute the voltage dependent elastic distortion of the liquid crystal elastic constants of $K_{11} = 1.14 \times 10^{-11}$ N, $K_{22} = 0.66 \times 10^{-11}$ N and $K_{33} = 1.82 \times 10^{-11}$ N and low frequency relative permittivities of $\varepsilon_{//} = 19.50$ and $\varepsilon_{\perp} = 5.40$ are used. Then using a liquid crystal layer of thickness $d = 6.00$ μm with ordinary and extraordinary indices of $n_e = 1.7400$, $n_o = 1.5200$ ($\Delta n = 0.22$) respectively for *x*-polarization incident the voltage dependent intensities and phases of the two transmitted components, T_{xx}, T_{xy} and Φ_x, Φ_y, are computed as shown in Figs. 2(a) and (b), respectively. It is very clear that even though T_{xx}, T_{xy} and Φ_x, Φ_y vary with voltage the phase difference between the output *x*- and *y*-polarizations is always $\pi/2$, i.e. $|\Phi_x - \Phi_y| = \pi/2$.
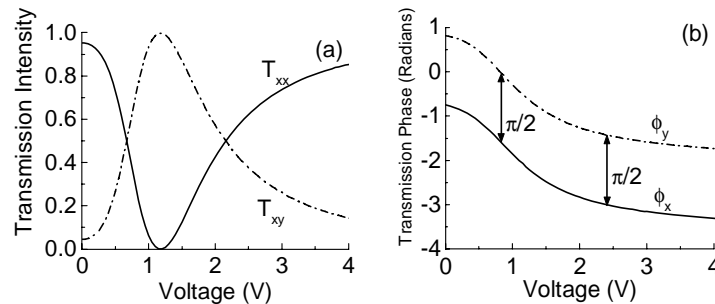

Fig. 2. The model results for a HAN cell under an applied voltage. The liquid crystal layer has $n_e = 1.7400$, $n_o = 1.5200$ and $d = 6.00$ μm. (a) The transmission intensities, T_{xx} and T_{xy} against voltage. (b) The transmission phases, Φ_x and Φ_y, against voltage.

Changing the liquid crystal layer thickness to $d = 8.00$ μm leads to the output phases Φ_x and Φ_y shown in Fig. 3(a) while using $d = 6.00$ μm and different optical anisotropy with $n_e = 1.7400$, $n_o = 1.5800$ ($\Delta n = 0.16$) gives the phases shown in Fig. 3(b). It is once more clear that even though the values of Φ_x and Φ_y are varying differently with voltage the phase difference, $|\Phi_x - \Phi_y|$, is always $\pi/2$.
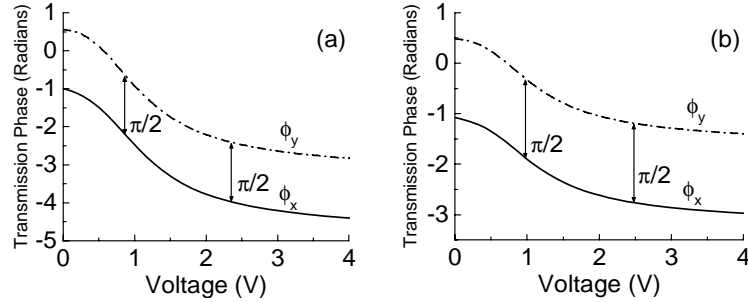
Fig. 3 The model results of a HAN cell under an applied voltage. The transmission phases, Φ_x and Φ_y, against voltage when the liquid crystal layer has (a) $n_e = 1.7400$, $n_o = 1.5200$ and $d = 8.00\ \mu m$ and (b) $n_e = 1.7400$, $n_o = 1.5800$ and $d = 6.00\ \mu m$.

4. Experiment

Two nematic liquid crystal cells have been built to test the above results, one is parallel aligned and the other is hybrid aligned. ITO coated glass plates with index 1.5170 have been used as cell walls. For the parallel aligned cell both inner surfaces of the glass plates are first coated in a thin layer of polyimide which is then uni-directionally rubbed. For the HAN cell the inner surface of one glass plate is coated with lecithin for homeotropic alignment while the other is prepared as for the parallel aligned cell. Two mylar strips with thickness about 6.0 μm are used as the cell gap spacers and then the cell is capillary filled with the liquid crystal (E7, Merck-BDH) at room temperature. The experimental set-up is shown in Fig. 4.
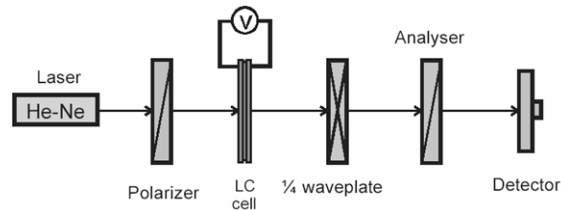

Fig. 4. The experimental set-up.

A 632.8 nm beam of radiation from a He-Ne laser is polarized along the *x*-axis. Either cell then follows with the plane containing the director set at 45° to the polarization plane of the incident radiation. A quarter-wave plate set to compensate for the $\pi/2$ phase difference between *x*- and *y*- output polarizations is then inserted. This is followed by an analyzer and detector to check the linearity of the final polarization state and to determine the polarization direction and intensity as a function of applied voltage.

Figure 5 shows the variation of the direction of the final linearly polarized beam as a function of applied voltage for the parallel and HAN aligned cells. As expected Fig. 5(a) shows a clear threshold at about 1 volt (rms, 5 kHz) corresponding to the Freederickz transition. By contrast Fig. 5(b) shows no threshold for the HAN cell and that 2π polarization rotation is readily achieved for a voltage range of less than 2 volts.

Figures 6(a) and (b) show the variation of output intensity as a function of voltage for the two cells. It is expected from modeling that there would be no variation of the output intensity with voltage. However while this is very closely true, there is a residual variation of order 3% for both types of cell. This is due to differences in absorption of the two polarization states by the quartz quarter-wave plate and analyzer and the multi-reflections from the various partially reflecting surfaces of the arrangement. For critical device applications anti-reflection coatings may be required to obviate these weak effects.
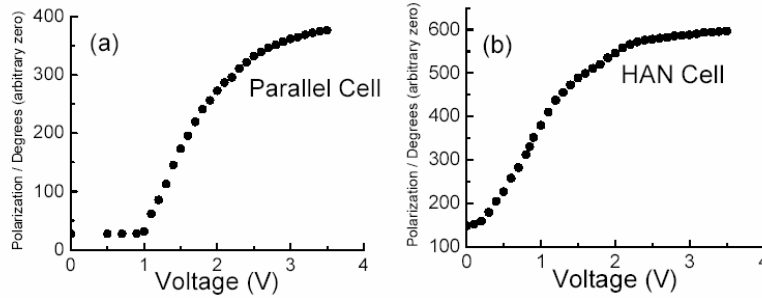
Fig. 5. The polarization direction of the output beam against applied voltage for (a) a parallel aligned cell and (b) a HAN cell.
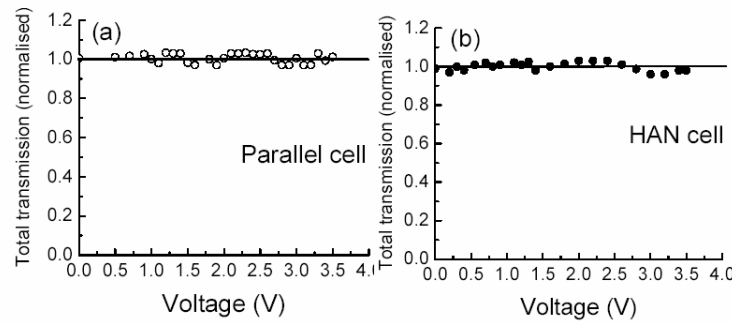

Fig. 6. Sum of transmissivities against applied voltage for (a) a parallel cell and (b) a HAN cell.

5. Conclusion

The basic unit of a polarization modulator is a polarization rotator which allows the transmitted radiation to be of linear polarization with fixed intensity which may have its direction of polarization controlled. For a liquid crystal cell having simple parallel or HAN geometry with no twist but with the director everywhere at 45° relative to the incident plane of polarization then for either pure x- or y-polarization incident the output radiation will always have a phase difference of $\pi/2$ between its x- and y-polarization components, regardless of the director tilt variation through the whole cell. Thus a quarter-wave plate placed behind the cell will give linearly polarized output. Under the application of a voltage to the cell the director of the liquid crystal tilts and the amount of x to y polarization conversion changes. Thereby the direction of polarization after the quarter-wave plate will vary with the external applied voltage. This combination provides the ideal polarization rotator. Since the liquid crystal director in a HAN cell is very easily controlled by small applied voltages and has a thresholdless response it is also easy to fabricate a programmable pixelated spatial light modulator. Thus the polarization-only modulator may be realized using a LC-SLM with the geometry mentioned above and to our knowledge this is the first time that such a geometry has been considered for a polarization rotator.

Acknowledgments